RSC Advances



PAPER

View Article Online
View Journal | View Issue



Cite this: RSC Adv., 2021, 11, 14148

Received 3rd February 2021 Accepted 31st March 2021

DOI: 10.1039/d1ra00900a

rsc.li/rsc-advances

Structure transition of a C_{60} monolayer on the Bi(111) surface

Ya-Ru Wang, Min-Long Tao, **D* Ma Chao-Ke, Zi-Long Wang, Da-Xiao Yang, Ming-Xia Shi, Kai Sun, Ji-Yong Yang and Jun-Zhong Wang **D**

The interfacial structures of C_{60} molecules adsorbed on solid surfaces are essential for a wide range of scientific and technological processes in carbon-based nanodevices. Here, we report structural transitions of the C_{60} monolayer on the Bi(111) surface studied *via* low-temperature scanning tunneling microscopy (STM). With an increase in temperature, the structure of the C_{60} monolayer transforms from local-order structures to a ($\sqrt{93} \times \sqrt{93}$) R20° superstructure, and then to a (11 \times 11) R0° superstructure. Moreover, the individual C_{60} molecules in different superstructures have different orientations. C_{60} molecules adopt the 6 : 6 C–C bond and 5 : 6 C–C bond facing-up, mixed orientations, and hexagon facing-up in the local-order structure, ($\sqrt{93} \times \sqrt{93}$) R20°, and (11 \times 11) R0° superstructure, respectively. These results shed important light on the growth mechanism of C_{60} molecules on solid surfaces.

Introduction

C₆₀ molecule, as a prototypical fullerene molecule, has attracted widespread attention due to its potential in endohedral fullerenes,1 photovoltaic devices,2 peapod nanotubes,3 and singlemolecule transistors.4 A C60 monolayer grown on solid surfaces is critical for understanding and controlling the interfacial properties of fullerene-derived electronic and photovoltaic devices. 5,6 STM studies demonstrated that the C₆₀ monolayer on the solid surface exhibit a variety of lattice orientations such as the "in phase" $(2\sqrt{3} \times 2\sqrt{3}) \text{ R}30^{\circ},^{7-13}, (7 \times 2\sqrt{3}) \text{ R}30^{\circ},^{7-13}$ 7) $R0^{\circ 13}$ and $(\sqrt{589} \times \sqrt{589})$ R14.5°. 13-15 The individual molecules of fullerene and fulleride within a single domain display different orientations. In the complex orientational ordering (7 \times 7) R0 $^{\circ}$ structure, a 7-molecule C₆₀ cluster consists of a central molecule sitting atop of a gold atom and six tilted surrounding molecules. In the unit cell of the ($\sqrt{589} \times \sqrt{589}$) R14.5° structure, 49 C_{60} molecules adopt 11 different orientations. ¹⁴ In the $(2\sqrt{3} \times 2\sqrt{3})$ R30° structure, all C₆₀ molecules are in the same orientation.12,16 The complex chiral motifs have been observed.17 In CsnC₆₀ fulleride films, orientational ordering appears.18 Moreover, "bright" and "dim" molecules have been widely found in the C₆₀ monolayer.⁹⁻¹⁷ However, the "dim" molecules in superstructures reported so far arrange irregularly.

The structure of C_{60} monolayers grown on the solid surface is not only related to C_{60} molecules themselves but also the substrate. In the past reports, there have been a large number of investigation on the C_{60} monolayer structures grown on numerous metals or semiconducting substrates, such as

School of Physical Science and Technology, Southwest University, Chongqing, China. E-mail: taotaole@swu.edu.cn; jzwangcn@swu.edu.cn

Ag, $^{7-9,19,20}$ Au, $^{10-16,21,22}$ Cu, $^{23-25}$ graphene, 26,27 Si, 28,29 Ge, 30 C₆₀, 29 or NaCl. 31 However, few reports address the superstructure of C₆₀ molecules adsorbed on semi-metal substrates. It is found that thin films of organic molecules grown on a semi-metallic Bi(111) surface shows a lot of interesting phenomena, such as the ordered crystalline layer with the standing-up orientation of pentacene molecules, 32 the chiral self-assembly of rubrene molecules, 33 structural transitions in different monolayers of cobalt phthalocyanine films, 34 and the Moire' pattern in C₆₀ thin films. 35

In this study, we use Bi(111) as the substrate and studied the structure transition of the C_{60} monolayer. C_{60} molecules were deposited at 100 K form local-order structures. When the deposition temperature increased to room temperature, the local-order structures turn into a long-range ordered ($\sqrt{93} \times \sqrt{93}$) R20° superstructure. After annealing at 400 K, the ordered superstructure transforms into the (11 \times 11) R0° superstructure. These superstructures are different from the structures of the C_{60} monolayer reported so far. Furthermore, the individual C_{60} molecules in the local-order structure, ($\sqrt{93} \times \sqrt{93}$) R20° and (11 \times 11) R0° superstructure, show the 6 : 6 C–C bond and 5 : 6 C–C bond facing-up, mixed orientations, and hexagon facing-up, respectively. The 6 : 6 (5 : 6) C–C bond indicates the common side of two adjacent hexagons (pentagon and hexagon) in C_{60} molecules.

Experimental

The experiments were conducted in an ultra-high vacuum low-temperature scanning tunneling microscope produced by Unisoku. The base pressure was kept at $\sim 1.2 \times 10^{-10}$ Torr. An Si(111) substrate was continuously degassed at ~ 870 K for 8 h

with subsequent flashing to 1400 K for several seconds. The Bi(111) film was prepared by depositing 20 monolayers of bismuth atoms on a Si(111)-7 \times 7 surface at room temperature with subsequent annealing at 400 K.³⁶ C₆₀ molecules were deposited onto the Bi(111) surface by heating the tantalum cell to 700 K. The growth rate of C₆₀ molecules was about 0.4 monolayers per minute. All STM images were acquired with a tungsten tip in constant-current mode at liquid nitrogen temperature (78 K).

Results and discussion

First, a small number of C_{60} molecules were deposited onto the Bi(111) surface when the substrate was maintained at 100 K. Fig. 1(a) shows the atomic-resolution image of the hexagonal lattices of the Bi(111) thin film. The lattice constants of the Bi(111) surface are measured to be $a_1=a_2=0.45\pm0.02$ nm, very close to the bulk value (a=0.454 nm) in Bi crystals. Fig. 1(b) shows the isolated C_{60} molecules on the Bi(111) surface presenting round protrusions. When reducing the bias voltage, the round protrusions are separated into two asymmetrical [Fig. 1(c)] or symmetrical [Fig. 1(d)] lobes, corresponding to the two different adsorption configurations, 5:6 C–C bond facing-up and 6:6 C–C bond facing-up, similar to C_{60} molecules on Au(111). This indicates that there are two stable adsorption orientations of isolated C_{60} molecules on the Bi(111) substrate, 6:6 C–C bond, and 5:6 C–C bond facing-up.

When the coverage increases, C_{60} molecules form the close-packed hexagonal structure, as shown in Fig. 2. We noticed that all the C_{60} molecules present a uniform height, except a few dim molecules (marked by green dotted circles). The brightness contrast in images stems from the different adsorption sites of C_{60} molecules. It is well known that metal surfaces do not behave as rigid templates for the chemisorption of C_{60} molecules, but may reconstruct substantially to accommodate the molecules. We speculate that Dim C_{60} molecules are located at

the vacancies of the Bi(111) substrate, originating from the reconstruction of the Bi(111) surface, similar to C_{60} molecules on Au(111)¹⁶ and Cu(111).³⁸

According to the arrangement of bright and dim molecules, we can see some local-order structures, though there is a lack of long-range ordering. In Fig. 2(a), there is an (11×8) R0° localorder structure (marked by red parallelogram). The lattice directions of (11×8) R0° are along with the directions of Bi(111), and the measured lattice constants are 5.00 \pm 0.02 nm and 3.64 \pm 0.02 nm, corresponding to 11 and 8 times of the lattice constant of the Bi(111) surface. The lattice directions of Bi(111) were obtained on the surface, which was not covered with C_{60} molecules. In another domain, shown in Fig. 2(b), the local-order structure is mixed with three types of structures, namely (11 \times 8) R0° (red quadrilateral), (11 \times 11) R0° (white quadrilateral), and (10 \times 8) R10 $^{\circ}$ (blue quadrilateral). In particular, we noticed that C₆₀ molecules exhibit almost the same orientation in a single domain, and most of the individual C₆₀ molecules in the local-order structure adopt two favorite orientations (6:6 C-C bond and 5:6 C-C bond facing up) as the isolated molecules on Bi(111). For example, most of the molecules shown in Fig. 2(a) present two symmetrical lobes, corresponding to C₆₀ molecules with a 6:6 C-C bond facing up. However, in Fig. 2(b), the molecules present two asymmetric lobes, corresponding to the 5:6 C-C bond facing up. We suggest that the formation of a local-order structure is due to the low-temperature growth. Because of the low kinetic energy of C₆₀ molecules at 100 K, molecular mobility is not high enough to form a long-range ordered superstructure. The C₆₀ molecules adsorbed on Bi(111) adopt their preferred orientations (6:6 C-C bond and 5:6 C-C bond facing up), similar to the isolated molecules adsorbed on the substrate. This proves the strong molecule-substrate interaction in the local-order structure.

To investigate the influence of temperature on the structure, we deposited C_{60} molecules on Bi(111) at room temperature. It

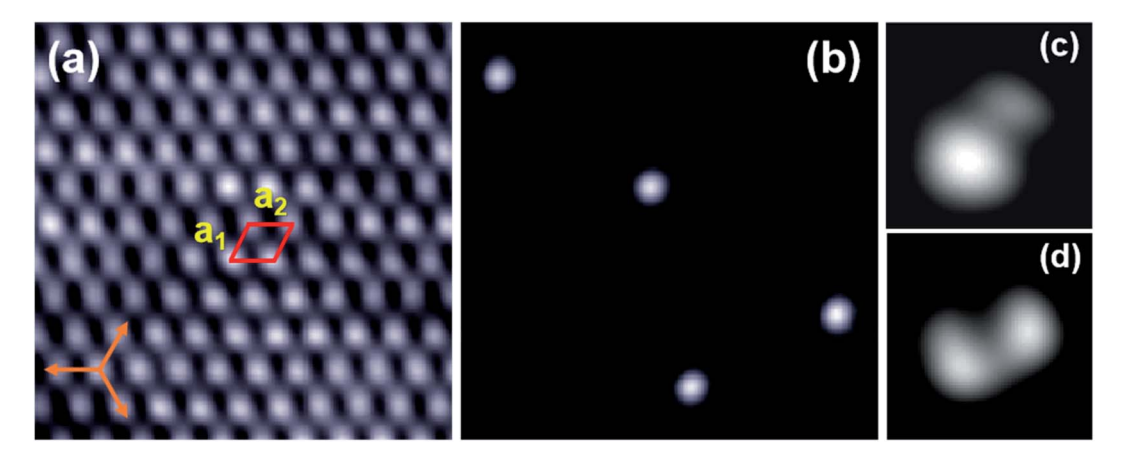


Fig. 1 The initial stage of C_{60} molecules adsorbed on the Bi(111) surface. (a) Hexagonal lattices of the Bi(111) surface, 5 nm \times 5 nm, -0.1 V. The unit cell is marked with a red box and the orange arrows indicate the directions of the Si(111) substrate. (b) Isolated C_{60} molecules adsorbed on Bi(111), 20 nm \times 20 nm, 2.2 V. (c) STM image of an isolated C_{60} molecule with two asymmetrical lobes corresponding to the 5 : 6 C–C bond facing up, 1.3 nm \times 1.3 nm, 400 mV. (d) STM image of an isolated C_{60} molecule with two symmetrical lobes corresponding to the 6 : 6 C–C bond facing up, 1.3 nm \times 1.3 nm, 200 mV.

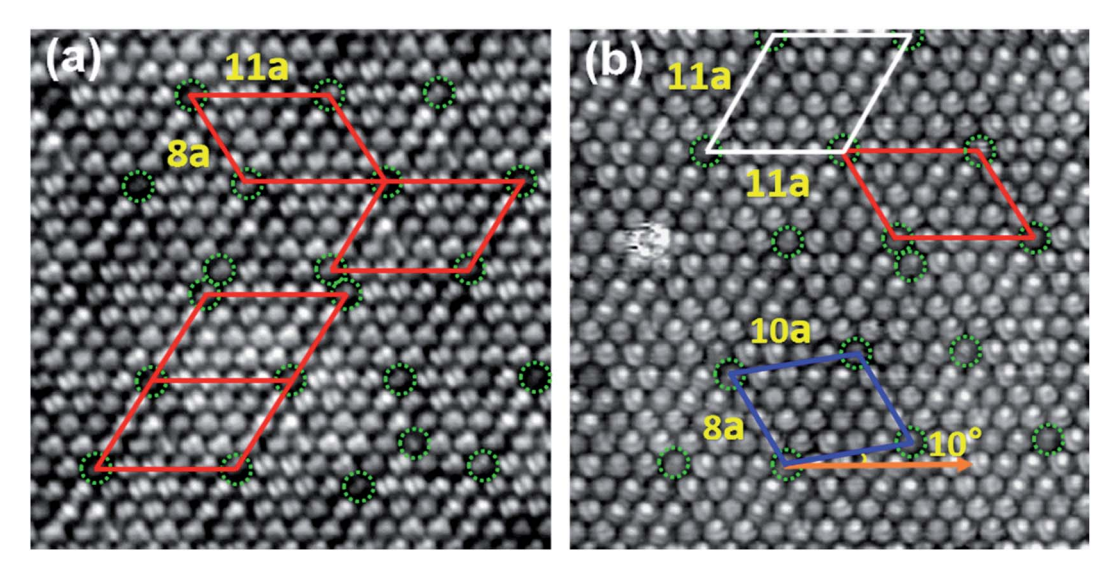


Fig. 2 Local-order structure in the monolayer C_{60} grown at a low temperature (\sim 100 K). (a) Four unit cells of the (11 \times 8) R0° superstructure appeared in the C_{60} monolayer, 20 nm \times 20 nm, -1.2 V. The dim C_{60} molecules, located at the hollow position of Bi(111), are marked by the green dotted circles. (b) The mixture of three types of superstructures, 20 nm \times 20 nm, -0.9 V. The red, white, and blue unit cells correspond to the superstructure (11 \times 8) R0°, (11 \times 11) R0°, and (10 \times 8) R10°.

is found that C_{60} molecules aggregate into a hexagonal structure, the same as C_{60} molecules in the local-order structure. However, the local-order structures, originating from the dim and bright molecules, turn into a long-range ordered ($\sqrt{93} \times \sqrt{93}$) R20° superstructure [Fig. 3(a)]. This superstructure is different from the structures of the C_{60} monolayer reported so far. There is a misorientation angle of 20° between the lattice directions of the C_{60} monolayer and the Bi(111) surface. The measured lattice constants of ($\sqrt{93} \times \sqrt{93}$) R20° are $b_1 = b_2 = 4.38 \pm 0.02$ nm, agreeing well with $\sqrt{93}$ times the lattice constant of Bi(111) (0.45 nm). Fig. 3(b) shows the schematic of the ($\sqrt{93} \times \sqrt{93}$) R20° superstructure. Based on the lattice constant of the Bi(111) substrate, the lattice vectors of the ($\sqrt{93} \times \sqrt{93}$) R20° superstructure can be expressed as following matrixes:

$$\begin{pmatrix} b_1 \\ b_2 \end{pmatrix} = \begin{pmatrix} 11 & -4 \\ 4 & 7 \end{pmatrix} \begin{pmatrix} a_1 \\ a_2 \end{pmatrix}$$

This ordered superstructure implies two things: first, the intermolecular interaction is getting stronger than that in the local-order structure prepared at low temperature (100 K). Second, the molecule–substrate interaction is also strong since the orientations of the C_{60} superstructure are commensurate with those of the substrate. Furthermore, we can clearly see that individual C_{60} molecules adopt various orientations, rather than the favorite orientations as C_{60} molecules in the local-order structure. As shown in the high-resolution STM image [Fig. 3(c)], C_{60} molecules in ($\sqrt{93} \times \sqrt{93}$) R20° present various shapes, such as two asymmetric lobes (white circle), two symmetrical lobes (yellow circle), and three lobes (blue circle),

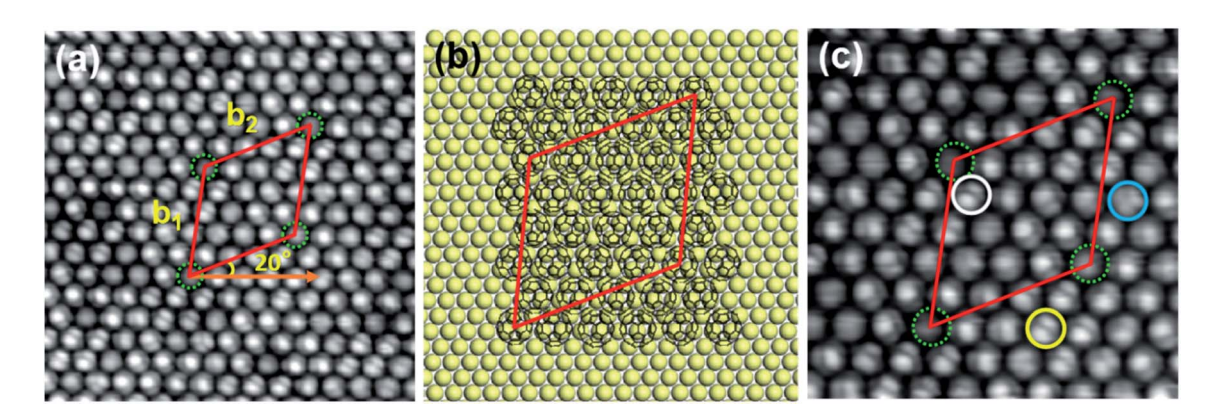


Fig. 3 (a) The STM image of the ($\sqrt{93} \times \sqrt{93}$) R20° superstructure, 15 nm \times 15 nm, -1.2 V. (b) Schematic model of the ($\sqrt{93} \times \sqrt{93}$) R20° superstructure. The yellow balls and black hollow balls represent Bi atoms and C₆₀ molecules. (c) High-resolution STM image of the ($\sqrt{93} \times \sqrt{93}$) R20° superstructure, 10 nm \times 10 nm, -1.0 V. The individual molecules exhibit different orientations, such as 5 : 6 C–C bond, 6 : 6 C–C bond, and hexagon facing up, marked by white, yellow, and blue solid circles, respectively.

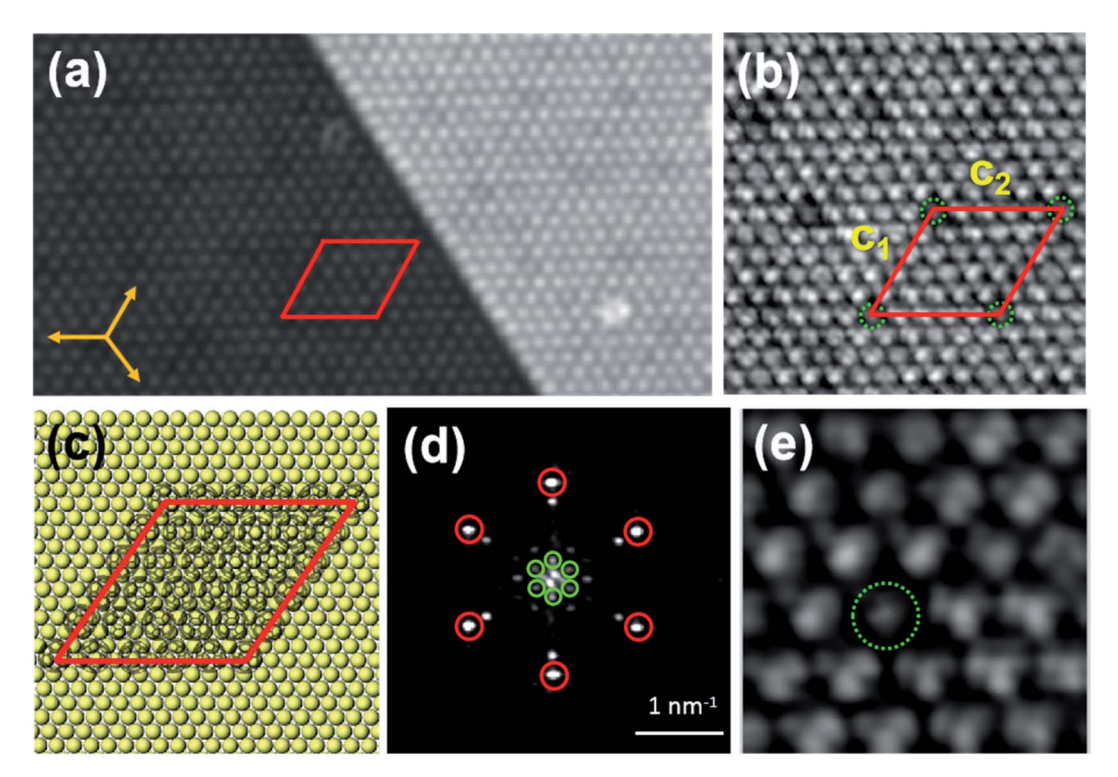


Fig. 4 (a) The STM image of the (11 \times 11) R0° superstructure corresponding to the Bi(111), 39 nm \times 21 nm, -1.5 V. (b) Close-up view of the (11 \times 11) R0° superstructure, 14 nm \times 14 nm, -0.7 V. (c) Schematic model of the (11 \times 11) R0° superstructure with respect to the Bi(111) lattices. (d) FFT of the image (a). The spots marked by red circles correspond to the C_{60} hexagonal lattices, while the spots marked by the green circles represent the (11 imes 11) R0 $^{\circ}$ superstructure. (e) STM image with a sub-molecular resolution of the superstructure, 5 nm imes 5 nm, -0.7 V.

corresponding to the 5:6 C-C bond, 6:6 C-C bond, and hexagon facing up. The diversity of C₆₀ molecular orientations is due to the enhancement of intermolecular interaction in the $(\sqrt{93} \times \sqrt{93})$ R20° superstructure. The intermolecular interaction enables C₆₀ molecules to overcome the molecule-substrate interaction and adopt other orientations, and then make the $(\sqrt{93} \times \sqrt{93})$ R20° superstructure stable.

When annealed at 400 K for about 20 min, C_{60} molecules still revealed a hexagonal lattice, while the superstructure transformed from $(\sqrt{93} \times \sqrt{93})$ R20° into (11×11) R0° superstructure [Fig. 4(a)], indicating that (11 \times 11) R0° is more stable than $(\sqrt{93} \times \sqrt{93})$ R20°. The lattice directions of (11×11) R0° are along the directions of the Bi(111) substrate, and the lattice constants are $c_1 = c_2 = 5.00 \pm 0.02$ nm [Fig. 4(b)], corresponding to 11 times of the lattice constant of Bi(111). Fig. 4(d) is the fast Fourier transform (FFT) image of the (11 \times 11) R0 $^{\circ}$ superstructure, where the spots marked by red and green circles correspond to C_{60} hexagonal lattices and the (11 \times 11) $R0^{\circ}$ superstructure. In the FFT image, the spots of the superstructure are clearly visible, though they are dimmer than the spots of C_{60} hexagonal lattices, implying that the (11 \times 11) $R0^{\circ}$ superstructure has long-range order. The schematic model of (11×11) R0° is shown in Fig. 4(c). From STM images, the $(11 \times$ 11) R0° superstructure seems to have the same structure as the reported structure attributed to a Moire' pattern in ref. 36. However, in our experiment, the (11 \times 11) $R0^{\circ}$ superstructure is transformed from the ($\sqrt{93} \times \sqrt{93}$) R20° superstructure and have no relationship with the Moire' pattern. From the close-up view of the $(11 \times 11) \text{ R0}^{\circ}$ superstructure in Fig. 4(e), it is found that all the C₆₀ molecules reveal a unified three-lobe structure, corresponding to the hexagon facing up, different from favorite orientations in the local-order structure and mixed orientations in $(\sqrt{93} \times \sqrt{93})$ R20°. With an increase in temperature, the superstructure of the C60 monolayer changes from local order to long-range order and C₆₀ molecules are re-orientated. This is because the thermal diffusivities of C₆₀ molecules and Bi atoms increase with the increase in temperature, which is conducive to the formation of a more orderly and stable superstructure.

Conclusions

In summary, the structure of C₆₀ molecules on Bi(111) changes with temperature variation. When deposited on the Bi(111) surface at 100 K, C_{60} molecules form local-order structures, and the molecules in local-order structures adopt their favorite orientations. As the deposition temperature increases to room temperature, the local-order structures turn into a long-range ordered ($\sqrt{93} \times \sqrt{93}$) R20° superstructure. The orientations of C_{60} molecules in ($\sqrt{93} \times \sqrt{93}$) R20° superstructures are diverse. After annealing at 400 K for about 20 min, the C₆₀ film exhibits a (11 \times 11) R0 $^{\circ}$ superstructure, and all C₆₀ molecules in this superstructure take the unified orientation, hexagon facing-up. The appearance of numerous superstructures and the molecular orientations in superstructures is due to the change in the

thermal diffusivity of C_{60} molecules and Bi atoms at different temperatures.

Conflicts of interest

There are no conflicts to declare.

Acknowledgements

This work was supported by the National Natural Science Foundation of China (Grant Nos. 11804282, 11874304, 11574253).

References

- 1 T. Ohtsuki, K. Masumoto, K. Ohno, Y. Maruyma, Y. Kawazoe, K. Sueki and K. Kikuchi, Insertion of Be Atoms in C₆₀ Fullerene Cages: Be@C₆₀, *Phys. Rev. Lett.*, 1996, 77, 3522.
- 2 C. Deibel and V. Dyakonov, Polymer-fullerene bulk heterojunction solar cells, *Rep. Prog. Phys.*, 2010, 73, 096401.
- 3 D. J. Hornbaker, S.-J. Kahng, S. Misra, B. W. Smith, A. T. Johnson, E. J. Mele, D. E. Luzzi and A. Yazdani, Mapping the One-Dimensional Electronic States of Nanotube Peapod Structures, *Science*, 2002, **295**, 828–831.
- 4 H. Park, J. Park, A. K. L. Lim, E. H. Anderson, A. P. Alivisatos and P. L. McEuen, Nanomechanical oscillations in a single-C₆₀ transistor, *Nature*, 2000, **407**, 57–60.
- 5 P. W. Stephens, G. Bortel, G. Faigel, M. Tegze, A. Jánossy, S. Pekker, G. Oszlanyi and L. Forró, Polymeric fullerene chains in RbC₆₀ and KC₆₀, *Nature*, 1994, 370, 636–639.
- 6 R. Yamachika, M. Grobis, A. Wachowiak and M. F. Crommie, Controlled atomic doping of a single molecule, *Science*, 2004, 304, 281–284.
- 7 H. I. Li, K. Pussi, K. J. Hanna, L. L. Wang, D. D. Johnson, H. P. Cheng, H. Shin, S. Curtarolo, W. Moritz and J. A. Smerdon, Surface Geometry of C₆₀ on Ag(111), *Phys. Rev. Lett.*, 2009, **103**, 056101.
- 8 K. Pussi, H. I. Li, H. Shin, L. N. S. Loli, A. K. Shukla, J. Ledieu, V. Fournee, L. L. Wang, S. Y. Su and K. E. Marino, Elucidating the dynamical equilibrium of C₆₀ molecules on Ag(111), *Phys. Rev. B: Condens. Matter Mater. Phys.*, 2012, **86**, 205426.
- 9 H. I. Li, G. J. P. Abreu, A. K. Shukla, V. Fournée, J. Ledieu, L. N. Serkovic Loli, S. E. Rauterkus, M. V. Snyder, S. Y. Su and K. E. Marino, Ordering and dynamical properties of superbright C₆₀ molecules on Ag(111), *Phys. Rev. B: Condens. Matter Mater. Phys.*, 2014, **89**, 085428.
- 10 L. Tang, Y. Xie and Q. Guo, Complex orientational ordering of C_{60} molecules on Au(111), *J. Chem. Phys.*, 2011, 135, 11470211.
- 11 X. Torrelles, M. Pedio, C. Cepek and R. Felici, $(2\sqrt{3} \times 2\sqrt{3})$ R30 degrees induced self-assembly ordering by C₆₀ on a Au(111) surface: X-ray diffraction structure analysis, *Phys. Rev. B: Condens. Matter Mater. Phys.*, 2012, **86**, 075461.
- 12 M. Passens, R. Waser and S. Karthaeuser, Enhanced fullerene-Au(111) coupling in $(2\sqrt{3} \times 2\sqrt{3})$ R30 degrees superstructures with intermolecular interactions, *Beilstein J. Nanotechnol.*, 2015, **6**, 1421–1431.

- 13 H. Shin, A. Schwarze, R. D. Diehl, K. Pussi, A. Colombier, E. Gaudry, J. Ledieu, G. M. McGuirk, L. N. S. Loli and V. Fournee, Structure and dynamics of C₆₀ molecules on Au(111), *Phys. Rev. B: Condens. Matter Mater. Phys.*, 2014, 89, 245428.
- 14 G. Schull and R. Berndt, Orientationally ordered (7 \times 7) superstructure of C_{60} on Au(111), *Phys. Rev. Lett.*, 2007, **99**, 226105.
- 15 X. Zhang, F. Yin, R. E. Palmer and Q. Guo, The C₆₀/Au(111) interface at room temperature: A scanning tunnelling microscopy study, *Surf. Sci.*, 2008, **602**, 885–892.
- 16 J. A. Gardener, G. A. D. Briggs and M. R. Castell, Scanning tunneling microscopy studies of C₆₀ monolayers on Au(111), Phys. Rev. B: Condens. Matter Mater. Phys., 2009, 80 235434
- 17 Y. Z. Shang, Z. L. Wang, D. X. Yang, Y. Y. Wang, C. K. Ma, M. L. Tao, K. Sun, J. Y. Yang and J. Z. Wang, Orientation ordering and chiral superstructures in fullerene monolayer on Cd(0001), *Nanomaterials*, 2020, 10, 1305.
- 18 S. Han, M. X. Guan, C. L. Song, Y. L. Wang, M. Q. Ren, S. Meng, X. C. Ma and Q. K. Xue, Visualizing molecular orientational ordering and electronic structure in CsnC₆₀ fulleride films, *Phys. Rev. B*, 2020, **101**, 085413.
- 19 W. W. Pai and C. L. Hsu, Ordering of an incommensurate molecular layer with adsorbate-induced reconstruction:C₆₀/Ag(100), *Phys. Rev. B: Condens. Matter Mater. Phys.*, 2003, **68**, 121403.
- 20 C. Grosse, O. Gunnarsson, P. Merino, K. Kuhnke and K. Kern, Nanoscale Imaging of Charge Carrier and Exciton Trapping at Structural Defects in Organic Semiconductors, *Nano Lett.*, 2016, 16, 2084–2089.
- 21 L. Tang, X. Zhang, Q. Guo, Y. Wu, L. Wang and H. Cheng, Two bonding configurations for individually adsorbed C₆₀ molecules on Au(111), *Phys. Rev. B: Condens. Matter Mater. Phys.*, 2010, 82, 125414.
- 22 L. Tang, X. Zhang and Q. Guo, Organizing C₆₀ molecules on a nanostructured Au(111) surface, *Surf. Sci.*, 2010, **604**, 1310–1314.
- 23 T. Hashizume, K. Motai, X. D. Wang, H. Shinohara, Y. Saito, Y. Maruyama, K. Ohno, Y. Kawazoe, Y. Nishina and H. W. Pickering, Intramolecular structures of C_{60} molecules adsorbed on the Cu(111)-(1 \times 1) surface, *Phys. Rev. Lett.*, 1993, **71**, 2959–2962.
- 24 S. Wong, W. W. Pai, C. Chen and M. Lin, Coverage-dependent adsorption superstructure transition of C₆₀/Cu(001), *Phys. Rev. B: Condens. Matter Mater. Phys.*, 2010, **82**, 125442.
- 25 G. Xu, X. Shi, R. Q. Zhang, W. W. Pai, H. T. Jeng and M. A. Van Hove, Detailed low-energy electron diffraction analysis of the (4×4) surface structure of C_{60} on Cu(111): Seven-atom-vacancy reconstruction, *Phys. Rev. B: Condens. Matter Mater. Phys.*, 2012, **86**, 075419.
- 26 G. Li, H. T. Zhou, L. D. Pan, Y. Zhang, J. H. Mao, Q. Zou, H. M. Guo, Y. L. Wang, S. X. Du and H. J. Gao, Selfassembly of C₆₀ monolayer on epitaxially grown, nanostructured graphene on Ru(0001) surface, *Appl. Phys. Lett.*, 2012, **100**, 0133041.

- 27 M. Jung, D. Shin, S. Sohn, S. Kwon, N. Park and H. Shin, Atomically resolved orientational ordering of C₆₀ molecules on epitaxial graphene on Cu(111), *Nanoscale*, 2014, **6**, 11835–11840.
- 28 J. G. Hou, J. L. Yang, H. Q. Wang, Q. X. Li, C. G. Zeng, H. Lin, W. Bing, D. M. Chen and Q. S. Zhu, Identifying molecular orientation of individual C_{60} on a Si(111)-(7 \times 7) surface, *Phys. Rev. Lett.*, 1999, **83**, 3001–3004.
- 29 H. Q. Wang, C. G. Zeng, B. Wang, J. G. Hou, Q. X. Li and J. L. Yang, Orientational configurations of the C_{60} molecules in the (2×2) superlattice on a solid C_{60} (111) surface at low temperature, *Phys. Rev. B: Condens. Matter Mater. Phys.*, 2001, **63**, 085417.
- 30 A. Goldoni, C. Cepek, M. De Seta, J. Avila, M. C. Asensio and M. Sancrotti, Interaction of C_{60} with Ge(111) in the $3\sqrt{3} \times 3\sqrt{3}$ R30° phase: A (2 × 2) model, *Phys. Rev. B: Condens. Matter Mater. Phys.*, 2000, **61**, 10411–10416.
- 31 J. Leaf, A. Stannard, S. P. Jarvis, P. Moriarty and J. L. Dunn, A combined monte carlo and huckel theory simulation of orientational ordering in C₆₀ assemblies, *J. Phys. Chem. C*, 2016, **120**, 8139–8147.
- 32 G. E. Thayer, J. T. Sadowski, F. M. z. Heringdorf, T. Sakurai and R. M. Tromp, Role of surface electronic structure in thin film molecular ordering, *Phys. Rev. Lett.*, 2005, **95**, 25510

- 33 K. Sun, M. Lan and J. Z. Wang, Absolute configuration and chiral self-assembly of rubrene on Bi(111), *Phys. Chem. Chem. Phys.*, 2015, 17, 26220.
- 34 M. L. Tao, Y. B. Tu, K. Sun, Y. Zhang, X. Zhang, Z. B. Li, S. J. Hao, H. F. Xiao, J. Ye and J. Z. Wang, Structural transitions in different monolayers of cobalt phthalocyanine film grown on Bi(111), *J. Phys. D: Appl. Phys.*, 2016, **49**, 015307.
- 35 J. T. Sadowski, R. Z. Bakhtizin, A. I. Oreshkin, T. Nishihara, A. Al-Mahboob, Y. Fujikawa, K. Nakajima and T. Sakurai, Epitaxial C_{60} thin films on Bi(0001), *Surf. Sci.*, 2007, **601**, 136–139.
- 36 T. Nagao, J. T. Sadowski, M. Saito, S. Yaginuma, Y. Fujikawa, T. Kogure, T. Ohno, Y. Hasegawa, S. Hasegawa and T. Sakurai, Nanofilm allotrope and phase transformation of ultrathin Bi film on Si(111)–7 × 7, *Phys. Rev. Lett.*, 2004, **93**, 105501.
- 37 X. Q. Shi, A. M. Van Hove and R. Q. Zhang, Survey of structural and electronic properties of C₆₀ on close-packed metal surfaces, *J. Mater. Sci.*, 2012, 47, 7341–7355.
- 38 W. W. Pai, H. T. Jeng, C. M. Cheng, C. H. Lin, X. Xiao, A. Zhao, X. Zhang, G. Xu, X. Q. Shi, M. A. Van Hove, C. S. Hsue and K. D. Tsuei, Optimal electron doping of a C₆₀ monolayer on Cu(111) via interface reconstruction, *Phys. Rev. Lett.*, 2010, **104**, 036103.